

**Diradicals** Hot PaperHow to cite: *Angew. Chem. Int. Ed.* **2022**, *61*, e202207415

International Edition: doi.org/10.1002/anie.202207415

German Edition: doi.org/10.1002/ange.202207415

# Isolation of an Arsenic Diradicaloid with a Cyclic C<sub>2</sub>As<sub>2</sub>-Core

Henric Steffenfauseweh, Yury V. Vishnevskiy, Beate Neumann, Hans-Georg Stammler, Diego M. Andrada, and Rajendra S. Ghadwal\*

Dedicated to Professor Wolfgang Schnick on the occasion of his 65th birthday

**Abstract:** Herein, we report on the synthesis, characterization, and reactivity studies of the first cyclic C<sub>2</sub>As<sub>2</sub>-diradicaloid {(IPr)CAs}<sub>2</sub> (**6**) (IPr = C{N(Dipp)CH}<sub>2</sub>; Dipp = 2,6-*i*Pr<sub>2</sub>C<sub>6</sub>H<sub>3</sub>). Treatment of (IPr)CH<sub>2</sub> (**1**) with AsCl<sub>3</sub> affords the Lewis adduct {(IPr)CH<sub>2</sub>}AsCl<sub>3</sub> (**2**). Compound **2** undergoes stepwise dehydrochlorination to yield {(IPr)CH}AsCl<sub>2</sub> (**3**) and {(IPr)CAsCl}<sub>2</sub> (**5a**) or [{(IPr)CAs<sub>2</sub>Cl}OTf] (**5b**). Reduction of **5a** (or **5b**) with magnesium turnings gives **6** as a red crystalline solid in 90% yield. Compound **6** featuring a planar C<sub>2</sub>As<sub>2</sub> ring is diamagnetic and exhibits well resolved NMR signals. DFT calculations reveal a singlet ground state for **6** with a small singlet-triplet energy gap of 8.7 kcal mol<sup>-1</sup>. The diradical character of **6** amounts to 20% (CASSCF, complete active space self consistent field) and 28% (DFT). Treatments of **6** with (PhSe)<sub>2</sub> and Fe<sub>2</sub>(CO)<sub>9</sub> give rise to {(IPr)CAs(SePh)}<sub>2</sub> (**7**) and {(IPr)CAs<sub>2</sub>Fe(CO)<sub>4</sub>} (**8**), respectively.

Molecules containing two unpaired electrons in two degenerate (or nearly degenerate) orbitals are regarded as diradicals.<sup>[1]</sup> Singlet diradicals (or diradicaloids) are of a particular significance because of their intriguing electronic structures<sup>[2]</sup> and reactivity.<sup>[3]</sup> On account of their auspicious optical, magnetic, and electronic properties,<sup>[4]</sup> these open-shell species have become highly sought-after candidates for their applications in the design of advanced molecular

materials.<sup>[5]</sup> Hence, the isolation and exploration of stable organic as well as main-group diradical(oid)s remains a highly avid research topic in fundamental chemistry.<sup>[6]</sup>

In 1995, Niecke et al. reported the first stable diradicaloid **I** (Figure 1).<sup>[7]</sup> In 2002, Bertrand et al. isolated a P<sub>2</sub>B<sub>2</sub>-diradicaloid **II**,<sup>[8]</sup> while a related aluminum species **III** was reported later by Schnöckel and co-workers.<sup>[9]</sup> Among Group 14 elements, Power (E = Ge),<sup>[10]</sup> Lappert (E = Sn),<sup>[11]</sup> and Sekiguchi (E = Si)<sup>[12]</sup> reported Niecke-type N<sub>2</sub>E<sub>2</sub>-diradicaloids **IV-E**. Over the last decade, Schulz and co-workers have isolated cyclic N<sub>2</sub>E<sub>2</sub>-diradicaloids **V-E** and **VI** (E = P or As)<sup>[13]</sup> and explored their electronic structures and reactivity.<sup>[6m,14]</sup> The stability of Niecke-type diradicaloids (**IV-E**)-(VI) may be attributed to the captodative (donor-acceptor) effect of nitrogen atoms.<sup>[15]</sup> Each of the nitrogen atoms of (**IV-E**)-(VI) contributes 2e to the N<sub>2</sub>E<sub>2</sub>-ring, giving rise to a formal Huckel's 4n+2 π-electron aromatic system.<sup>[16]</sup> While diradical character and aromaticity are not mutually exclusive,<sup>[17]</sup> compounds with a large diradical character are expected to be weak (or non-) aromatic.<sup>[6,18]</sup> In 2017, the research groups of Grützmacher<sup>[19]</sup> and Ghadwal<sup>[20]</sup> independently reported two different synthetic routes to a C<sub>2</sub>P<sub>2</sub>-diradicaloid **VII-P** based on an N-heterocyclic carbene (NHC), i.e. IPr (Figure 1). Note, the arsenic analogue **VII-As** remained, nonetheless, thus far unknown. This is most likely due to the limitation of available synthetic methods and/or the lack of suitable starting materials. Herein, we

[\*] H. Steffenfauseweh, Dr. Y. V. Vishnevskiy, B. Neumann, Dr. H.-G. Stammler, Priv.-Doz. Dr. R. S. Ghadwal  
Molecular Inorganic Chemistry and Catalysis, Inorganic and Structural Chemistry, Center for Molecular Materials, Faculty of Chemistry, Universität Bielefeld  
Universitätsstr. 25, 33615 Bielefeld (Germany)  
E-mail: rghadwal@uni-bielefeld.de  
Homepage: <http://www.ghadwalgroup.de>

Dr. D. M. Andrada  
Faculty of Natural Sciences and Technology, Department of Chemistry, Saarland University  
Campus C4.1, 66123 Saarbrücken (Germany)

© 2022 The Authors. *Angewandte Chemie International Edition* published by Wiley-VCH GmbH. This is an open access article under the terms of the Creative Commons Attribution Non-Commercial NoDerivs License, which permits use and distribution in any medium, provided the original work is properly cited, the use is non-commercial and no modifications or adaptations are made.

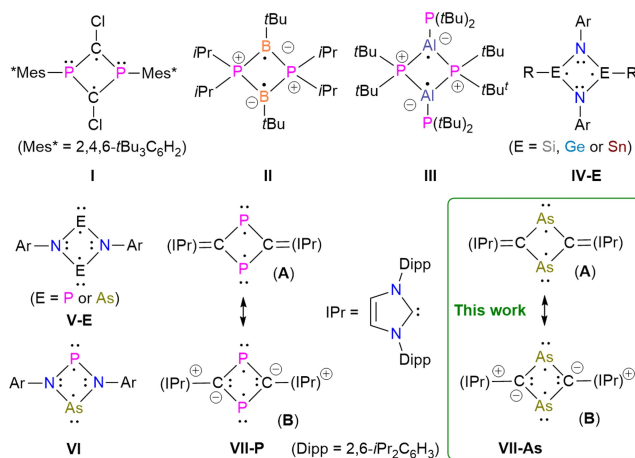


Figure 1. Selected examples of stable main-group singlet diradicals.

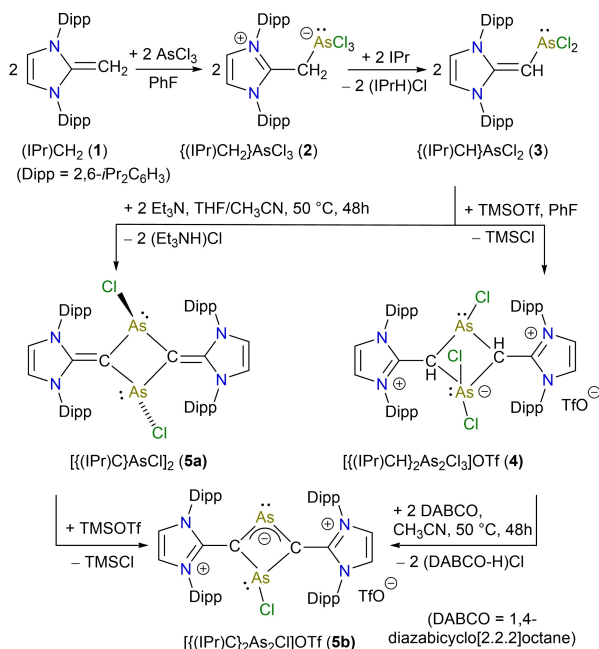
report the first  $C_2As_2$ -diradicaloid **VII-As** as a red crystalline solid.

Treatment of  $(IPr)CH_2$  (**1**) with  $AsCl_3$  affords the Lewis adduct  $\{(IPr)CH_2\}AsCl_3$  (**2**) as a colorless crystalline solid in 87% yield (Scheme 1). In THF, **2** readily undergoes dehydrochlorination with 1 equiv of IPr base to afford the N-heterocyclic vinyl (NHV)<sup>[21]</sup> derivative  $\{(IPr)CH\}AsCl_2$  (**3**). Compound **3** (lime green) has limited stability in solution as well as in the solid-state. Samples of **3** (both solid as well as solutions) turned dark green on storing them at room temperature overnight. <sup>1</sup>H NMR analyses of these samples indicated the formation of an intractable mixture of products including  $(IPrCH_3)Cl$  and some residual **3**. This suggests the auto-deprotonation of **3**, which can be rationalized by considering its Lewis basicity, like **1**, owing to the presence of highly polarizable vinylic bond. Nonetheless, **3** can be converted into a thermally stable dimer  $[(IPr)CHAsCl]_2Cl[OTf]$  (**4**) on treatment of a freshly pre-

pared PhF solution of **3** with TMSOTf. The dehydrochlorination of **3** is feasible with  $Et_3N$  to obtain **5a**, albeit in a low yield (39%). Treatment of an acetonitrile solution of **4** with DABCO at 50 °C for two days affords **5b** as a dark green solid in 90% yield. **5b** is also accessible by reacting **5a** with TMSOTf or KOTf. Compounds **2–5** exhibit expected <sup>1</sup>H and <sup>13</sup>C NMR signals for the IPr moiety (see the Supporting Information). The <sup>1</sup>H NMR spectrum of **2** shows a singlet at 3.06 ppm for the  $CH_2$  group. The <sup>1</sup>H NMR spectra of **3** (4.54 ppm) and **4** (3.35 ppm) show a singlet for the  $CHAs$  moiety.

The molecular structures **2** and **4** (Figure 2) exhibit the expected atom connectivity.<sup>[22]</sup> The C28–As1 bond length of the Lewis adduct **2** (2.015(2) Å) compares well with that of  $(IPr)AsCl_3$  (2.018(3) Å).<sup>[23]</sup> The  $C_{(IPr)}-C$  bond lengths of **2** (C1–C28: 1.480(2) Å) and **4** (C1–C2: 1.474(1) Å) are larger than that of  $(IPr)CH_2$  (**1**) (1.332(4) Å)<sup>[24]</sup> but consistent with the adducts of **1** with main-group Lewis acids (ca. 1.48 Å).<sup>[25]</sup> The molecular structure of **5a** (Figure 3) has an inversion center thus the other half of the molecule was symmetry generated. The chlorides were occupied at two positions with a long [As1–Cl1A (2.395(7) Å) and a short [As1–Cl1B (2.309(7) Å) As–Cl bond lengths. The four-membered  $C_2As_2$  ring of **5a** has a plane fold angle of 6.88(6)° from the nearly coplanar peripheral  $C_3N_2$ -rings. The C1–C4 (1.381(1) Å) and C4–As1 (1.909(1) Å) bond lengths of **5a** are smaller compared to those of **2** and **4**, suggesting a modest double bond character (see below for NBO analyses).<sup>[21,26]</sup>

Treatment of a THF solution of **5a** (or **5b**) with Mg turnings leads to the formation of compound **6** as a red crystalline solid (Scheme 2). **6** is indefinitely stable under inert gas atmosphere but readily decomposes when exposed to air. The <sup>1</sup>H and <sup>13</sup>C NMR spectra of **6** exhibit well-resolved signals due to the  $(IPr)C$  moiety. The <sup>1</sup>H NMR spectrum of **6** shows two doublets ( $Me_2CH$ ), one septet ( $Me_2CH$ ), and one singlet (NCH) for the IPr unit, indicating its highly symmetric structure.



**Scheme 1.** Synthesis of **2**, **3**, **4**, **5a**, and **5b**.

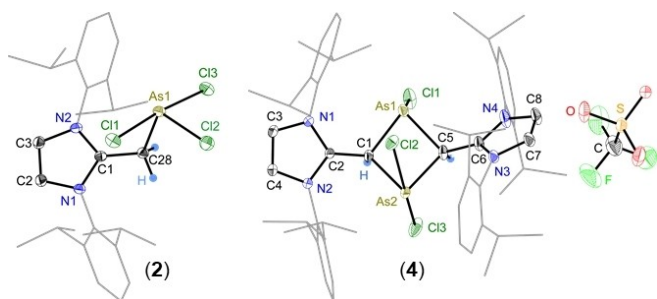


**Figure 2.** Molecular structures of **2** and **4**. Dipp groups are shown as wire-frame models. H atoms, except of CH or  $CH_2$  moiety, and solvent molecules are omitted for clarity. Thermal ellipsoids are depicted at 50% probability.

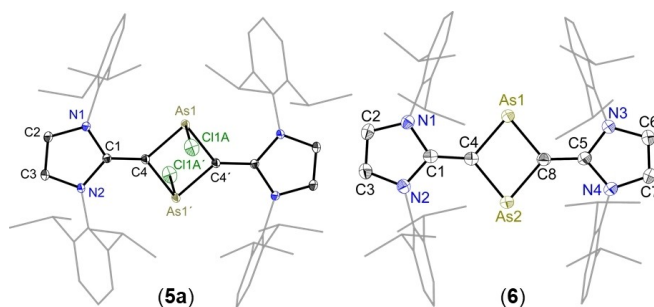
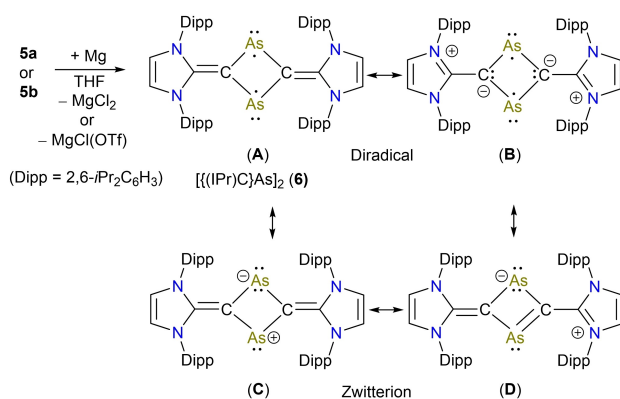


**Figure 3.** Solid-state molecular structures of **5a** and **6**. Dipp groups are shown as wire-frames and H atoms are omitted for clarity. Thermal ellipsoids are depicted at 50% probability. Selected bond lengths [Å] and bond angles [°] for **5a**: As–Cl1A 2.395(7), As–Cl1B 2.309(7) (structure has one long and one short As–Cl distances, only long one with Cl1A are shown), As1–C4 1.909(1), C1–C4 1.381(1); Cl1A–As1–C4 97.7(2), C4–As1–C4' 80.9(1), As1–C4–As1' 99.1(1). For **6**: As1–C4 1.919(2), As1–C8 1.921(2), As2–C4 1.907(2), As2–C8 1.914(2), C1–C4 1.380(3), C8–C5 1.376(3); C4–As1–C8 79.1(1), C4–As2–C8 79.6(1), As1–C4–As2 100.8(1), As1–C8–As2 100.5(1).



**Scheme 2.** Reduction of **5a** (or **5b**) with magnesium (turnings) to **6** with representative diradical (**A** and **B**) and zwitterion (**C** and **D**) resonance forms.

The molecular structure of **6** (Figure 3) features a planar  $\text{C}_2\text{As}_2$  ring that is twisted by  $4.09(9)^\circ$  and  $2.89(10)^\circ$  from the nearly coplanar peripheral  $\text{C}_3\text{N}_2$ -rings. The trans-annular  $\text{As}1\cdots\text{As}2$  interatomic distance of **6** ( $2.948(2)\text{ \AA}$ ) is larger than the sum of the arsenic covalent radii ( $2.42\text{ \AA}$ ) but smaller than the sum of the van der Waals radii ( $3.70$ ).<sup>[27]</sup> The  $\text{As}1\text{---C}4/\text{As}1\text{---C}8$  ( $1.915(2)/1.921(2)\text{ \AA}$ ) and  $\text{C}1\text{---C}4/\text{C}5\text{---C}8$  ( $1.380(3)/1.376(3)\text{ \AA}$ ) bond lengths of **6** are comparable to those of **5a** ( $1.909(1)$ ,  $1.381(1)\text{ \AA}$ , respectively). They are also similar to those of divinylarsene  $[(\text{IPr})\text{C}(\text{Ph})\text{As}]_2$  ( $1.919(1)$ ,  $1.376(2)\text{ \AA}$ ) comprising a  $\pi$ -conjugated linear  $\text{C}_2\text{As}_2\text{C}_2$ -framework.<sup>[28]</sup>

Further insight into the electronic structure of **6** was obtained by theoretical calculations. The DFT optimized structure of **6** at the RKS-PBEh-3c level of theory (Figure S35) is in good agreement with the XRD structure (Figure 3). We performed NBO (natural bond orbital) analyses for **1**, **2**, **5a**, and **6** (see the Supporting Information). The calculated Wiberg bond indices (WBIs) for the  $\text{C}1\text{---C}4$  (**5a** 1.41; **6** 1.37) and  $\text{C}4\text{---As}1$  (**5a** 0.95; **6** 1.02) bonds are consistent with their bond lengths (Figure 3). The NBO charges at the  $\text{C}1$  (**5a** 0.40; **6** 0.39),  $\text{C}4$  (**5a**  $-0.98$ ; **6**  $-0.85$ ), and  $\text{As}$  (**5a** 1.03; **6** 0.40) atoms indicate strongly polarized  $\text{C}1\text{---C}4$  bond and partial  $\pi$ -electron density transfer on to the arsenic atoms of the  $\text{C}_2\text{As}_2$  ring. For comparison, related details of compounds **1** (WBI for  $\text{C}1\text{---C}4$  1.62) and **2** (WBIs for  $\text{C}1\text{---C}4$  1.08,  $\text{C}4\text{---As}1$  0.78) are also provided in the Supporting Information (Tables S5–S7). As previously described for the phosphorus analogue **VII-P** (Figure 1),<sup>[19]</sup> compound **6** may also be viewed as an NHC-stabilized  $\text{C}_2\text{As}_2$ -cluster.<sup>[29]</sup>

The HOMO of **6** is a  $\pi$ -type orbital mainly located at the arsenic atoms of the  $\text{C}_2\text{As}_2$  ring and has trans-annular antibonding combination (Figure 4). The LUMO spans mainly over the  $\text{C}_2\text{As}_2\text{C}_2$ -framework with some contribution from the nitrogen atoms. Note that the LUMO has trans-annular bonding combination. These features are consistent with Niecek-type singlet  $\text{N}_2\text{E}_2$ -diradicals (**IV-E**)–(**VI**) (Figure 1). The HOMO–LUMO energy gap ( $\Delta E_{\text{H-L}} = 2.47\text{ eV}$ ) of **6** is rather small, suggesting its high reactivity (see below). The UV/Vis spectrum of **6** (Figure S26) exhibits three main

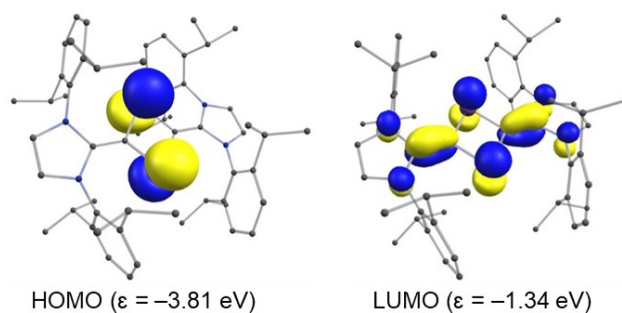
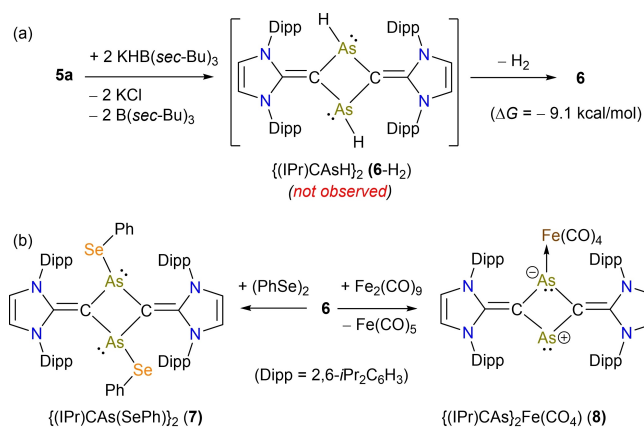


**Figure 4.** HOMO and LUMO of **6** (0.05 a.u. isosurface, PBE0/def2-TZVP).

absorptions ( $\lambda_{\text{max}}$ ) at 369, 519, and 655 nm, which based on TD-DFT calculations (Table S11) can be assigned to  $\text{HOMO}-1\rightarrow\text{LUMO}+9$ ,  $\text{HOMO}\rightarrow\text{LUMO}+7/\text{HOMO}-1\rightarrow\text{LUMO}$ , and  $\text{HOMO}\rightarrow\text{LUMO}$  transitions, respectively.

Despite the closed-shell singlet (**CS**) ground state, the singlet-triplet energy gap ( $\Delta E_{\text{S-T}} = 8.7\text{ kcal mol}^{-1}$ ) calculated for **6** at the PBEh-3c level of theory is fairly small. Interestingly, the broken-symmetry open-shell singlet (**OS**) solution for **6** is calculated to be  $0.34\text{ kcal mol}^{-1}$  lower in energy than the **CS** electronic state. The diradical character ( $\gamma$ ) according to Yamaguchi<sup>[30]</sup> is calculated to be 28%. The multireference SA-CASSCF(10,8)/def2-TZVP calculations reveal that the ground electronic state  $S_0$  has the active space occupation pattern 22222000 (88%) and 22220200 (10%). The diradical character ( $\beta$ ) for the CASSCF electronic structure  $S_0$  amounts to 20%. Like Niecek-type singlet diradicals **IV–VII** (Figure 1), **6** may also be regarded as a  $6\pi$  electron  $\text{C}_2\text{As}_2$  ring system. However, the calculated nuclear independent chemical shift (NICS) ( $\text{NICS}(1) = -3.4$ ;  $\text{NICS}(1)_{zz} = -0.1$ ) values indicate a rather weak aromatic character of the  $\text{C}_2\text{As}_2$  ring (Table S12, Figure S42). This is also consistent with the weak ring current at the  $\text{C}_2\text{As}_2$  ring of **6** as visualized by the ACID (anisotropy of the induced current density) plots (Figure S43).<sup>[31]</sup> Though aromaticity and diradical character are not mutually exclusive,<sup>[17]</sup> a rather weak aromaticity of **6** may account for the diradical character.<sup>[6,18]</sup>

Dihydrogen splitting is considered as a benchmark reaction of diradicals.<sup>[32]</sup> No change in the  $^1\text{H}$  NMR spectrum was observed upon exposure of a  $\text{C}_6\text{D}_6$  solution of **6** to  $\text{H}_2$  (1 atm) at room temperature. Warming this solution at  $80^\circ\text{C}$  for 2 h led to the decomposition of **6** as evident by the formation of  $(\text{IPr})\text{CH}_2$ . We attempted an alternative method for the preparation of the hydride **6-H}\_2** by reacting **5a** with  $\text{KHB}(\text{sec-Bu})_3$  (Scheme 3a). This reaction, however, afforded **6** and **1** instead of **6-H}\_2**. We assume that **6-H}\_2** is unstable and decomposes into **6** and  $\text{H}_2$ , which is calculated to be thermodynamically favored by  $9.1\text{ kcal mol}^{-1}$ . We also carried out low temperature  $^1\text{H}$  NMR studies of a reaction of **5a** and  $\text{KHB}(\text{sec-Bu})_3$ , which showed the formation of  $\text{H}_2$  already at 233 K (Figure S1). At 293 K, the  $^1\text{H}$  NMR spectrum indicates the presence of **6**, **1**, and  $\text{H}_2$  as sole reaction products.



**Scheme 3.** a) Reaction of **5a** with  $\text{KHB}(\text{sec-Bu})_3$  to **6**. b) Synthesis of **7** and **8**.

Reactions of **6** with  $(\text{PhSe})_2$  and  $\text{Fe}_2(\text{CO})_9$  afford compounds **7** and **8**, respectively (Scheme 3). Compounds **7** and **8** are stable solids and have been characterized by NMR spectroscopy, mass spectrometry, and single-crystal X-ray diffraction (Figure 5). The molecular structure of **7** shows the presence of  $\text{SePh}$  substituents at the arsenic atom in *cis*-fashion. In **7**, the C–C (1.377(4)/1.374(4) Å) and C–As (1.927(3)–1.936(3) Å) bond lengths of the  $\text{C}_2\text{As}_2$  ring are comparable to those of **5a**. As expected for unsymmetrically substituted  $\text{C}_2\text{As}_2$  ring in **8**, the As1–C4/As1–C8 (1.960(3)/1.964(3) Å) bond lengths are longer than As2–C7/As2–C8 (1.871(3)/1.881(3) Å). Thus, the latter have a partial multiple bond character, while the positive charge is formally distributed over the imidazole rings. The As–Fe bond length of **8** (2.475(1) Å) is larger than that of the electrophilic arsinidene complex  $\{(\text{IPr})\text{CPh}\}\text{As}\}\text{Fe}(\text{CO})_4$  (2.367(4) Å)<sup>[33]</sup> but compares well with four-coordinated nucleophilic arsinidene species (2.48 Å).<sup>[34]</sup>

In conclusion, the  $\text{C}_2\text{As}_2$ -diradicaloid **6** embedded between NHC (IPr) moieties has been isolated as a crystalline solid and characterized by spectroscopic and X-ray diffraction methods. Calculations suggest a singlet ground state for **6** with a considerably small singlet-triplet energy gap (8.7 kcal mol<sup>-1</sup>). The calculated diradical character of **6** amounts to 20% (CASSCF) and 28% (PUHF, projection

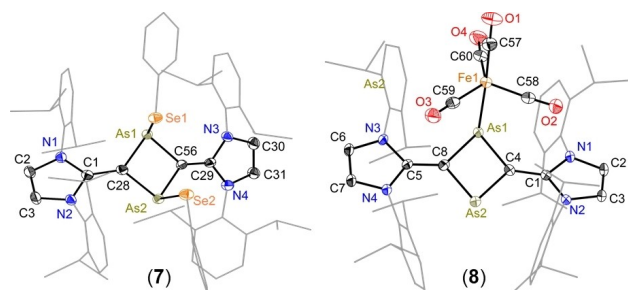


**Figure 5.** Solid-state molecular structures of **7** and **8**. H atoms have been omitted and aryl groups are shown as wireframe for clarity. Thermal ellipsoids are depicted at 50% probability.

unrestricted Hartree–Fock). Reactivity of **6** has been shown with  $(\text{PhSe})_2$  and  $\text{Fe}_2(\text{CO})_9$ , affording compounds **7** and **8**, respectively.

## Acknowledgements

We are grateful to the Deutsche Forschungsgemeinschaft (DFG, German Research Foundation) for generous support (GH 129/4-2, GH 129/9-1 and VI 713/1-3). The authors thank Professor Norbert W. Mitzel for continuous support. The HPC facilities at the Universität zu Köln are acknowledged for computing time and programs. Open Access funding enabled and organized by Projekt DEAL.

## Conflict of Interest

The authors declare no conflict of interest.

## Data Availability Statement

The data that support the findings of this study are available in the Supporting Information of this article.

**Keywords:** Arsenic • Carbenes • Diradicals • Heterocycles • Vinylidene Ligands

- [1] a) T. Stuyver, B. Chen, T. Zeng, P. Geerlings, F. De Proft, R. Hoffmann, *Chem. Rev.* **2019**, *119*, 11291–11351; b) M. Abe, *Chem. Rev.* **2013**, *113*, 7011–7088; c) L. Salem, C. Rowland, *Angew. Chem. Int. Ed. Engl.* **1972**, *11*, 92–111; *Angew. Chem.* **1972**, *84*, 86–106.
- [2] a) P. Coburger, R. Wolf, H. Grützmacher, *Eur. J. Inorg. Chem.* **2020**, 3580–3586; b) E. Miliordos, K. Ruedenberg, S. S. Xanthreas, *Angew. Chem. Int. Ed.* **2013**, *52*, 5736–5739; *Angew. Chem.* **2013**, *125*, 5848–5851.
- [3] a) M. Abe, J. Ye, M. Mishima, *Chem. Soc. Rev.* **2012**, *41*, 3808–3820; b) J. Michl, V. Bonačić-Koutecký, *Tetrahedron* **1988**, *44*, 7559–7585; c) Y. Jung, M. Head-Gordon, *ChemPhysChem* **2003**, *4*, 522–525.
- [4] a) J. J. Dressler, M. Teraoka, G. L. Espejo, R. Kishi, S. Takamuku, C. J. Gómez-García, L. N. Zakharov, M. Nakano, J. Casado, M. M. Haley, *Nat. Chem.* **2018**, *10*, 1134–1140; b) K. Fukuda, M. Nakano, *J. Phys. Chem. A* **2014**, *118*, 3463–3471.
- [5] a) L. Ji, J. Shi, J. Wei, T. Yu, W. Huang, *Adv. Mater.* **2020**, *32*, 1908015; b) E. Cho, V. Coropceanu, J.-L. Brédas, *J. Am. Chem. Soc.* **2020**, *142*, 17782–17786; c) W. W. Schoeller, *Eur. J. Inorg. Chem.* **2019**, 1495–1506; d) D. A. Wilcox, V. Agarkar, S. Mukherjee, B. W. Boudouris, *Annu. Rev. Chem. Biomol. Eng.* **2018**, *9*, 83–103; e) I. Ratera, J. Veciana, *Chem. Soc. Rev.* **2012**, *41*, 303–349; f) T. Ullrich, P. Pinter, J. Messelberger, P. Haines, R. Kaur, M. M. Hansmann, D. Munz, D. M. Guldi, *Angew. Chem. Int. Ed.* **2020**, *59*, 7906–7914; *Angew. Chem.* **2020**, *132*, 7980–7988; g) H. Guo, Q. Peng, X.-K. Chen, Q. Gu, S. Dong, E. W. Evans, A. J. Gillett, X. Ai, M. Zhang, D. Credgington, V. Coropceanu, R. H. Friend, J.-L. Brédas, F. Li, *Nat. Mater.* **2019**, *18*, 977–984; h) X. Ai, Y. Chen, Y. Feng, F. Li, *Angew. Chem. Int. Ed.* **2018**, *57*, 2869–2873; *Angew. Chem.* **2018**, *130*, 2919–2923; i) J. Messelberger, A. Grünwald, P. Pinter, M. M. Hansmann, D. Munz, *Chem. Sci.* **2018**, *9*, 6107–6117; j) S. Ito,

- T. Nagami, M. Nakano, *J. Photochem. Photobiol. C* **2018**, *34*, 85–120; k) D. López-Carballeira, D. Casanova, F. Ruipérez, *Phys. Chem. Chem. Phys.* **2017**, *19*, 30227–30238.
- [6] a) H. Grützmacher, F. Breher, *Angew. Chem. Int. Ed.* **2002**, *41*, 4006–4011; *Angew. Chem.* **2002**, *114*, 4178–4184; b) F. Breher, *Coord. Chem. Rev.* **2007**, *251*, 1007–1043; c) Y. Su, X. Wang, X. Zheng, Z. Zhang, Y. Song, Y. Sui, Y. Li, X. Wang, *Angew. Chem. Int. Ed.* **2014**, *53*, 2857–2861; *Angew. Chem.* **2014**, *126*, 2901–2905; d) G. He, O. Shynkaruk, M. W. Lui, E. Rivard, *Chem. Rev.* **2014**, *114*, 7815–7880; e) A. Hinz, R. Kuzora, U. Rosenthal, A. Schulz, A. Villinger, *Chem. Eur. J.* **2014**, *20*, 14659–14673; f) D. Rottschäfer, N. K. T. Ho, B. Neumann, H.-G. Stämmler, M. van Gastel, D. M. Andrada, R. S. Ghadwal, *Angew. Chem. Int. Ed.* **2018**, *57*, 5838–5842; *Angew. Chem.* **2018**, *130*, 5940–5944; g) D. Rottschäfer, B. Neumann, H.-G. Stämmler, D. M. Andrada, R. S. Ghadwal, *Chem. Sci.* **2018**, *9*, 4970–4976; h) S. Yoshidomi, M. Abe, *J. Am. Chem. Soc.* **2019**, *141*, 3920–3933; i) K. Chandra Mondal, S. Roy, H. W. Roesky, *Chem. Soc. Rev.* **2016**, *45*, 1080–1111; j) Z. Zeng, X. Shi, C. Chi, J. T. Lopez Navarrete, J. Casado, J. Wu, *Chem. Soc. Rev.* **2015**, *44*, 6578–6596; k) R. S. Ghadwal, *Synlett* **2019**, *30*, 1765–1775; l) S. González-Gallardo, F. Breher in *Comprehensive Inorganic Chemistry II*, 2nd ed. (Eds.: J. Reedijk, K. Poepplmeier), Elsevier, Amsterdam, **2013**, p. 413–455; m) J. Bresien, L. Eickhoff, A. Schulz, E. Zander, *Reference Module in Chemistry, Molecular Sciences and Chemical Engineering*, Elsevier, Amsterdam, **2021**; n) C. Helling, S. Schulz, *Eur. J. Inorg. Chem.* **2020**, 3209–3221.
- [7] E. Niecke, A. Fuchs, F. Baumeister, M. Nieger, W. W. Schoeller, *Angew. Chem. Int. Ed. Engl.* **1995**, *34*, 555–557; *Angew. Chem.* **1995**, *107*, 640–642.
- [8] D. Scheschkewitz, H. Amii, H. Gornitzka, W. W. Schoeller, D. Bourissou, G. Bertrand, *Science* **2002**, *295*, 1880–1881.
- [9] P. Henke, T. Pankewitz, W. Klopfer, F. Breher, H. Schnöckel, *Angew. Chem. Int. Ed.* **2009**, *48*, 8141–8145; *Angew. Chem.* **2009**, *121*, 8285–8290.
- [10] a) X. Wang, Y. Peng, M. M. Olmstead, J. C. Fettinger, P. P. Power, *J. Am. Chem. Soc.* **2009**, *131*, 14164–14165; b) C. Cui, M. Brynda, M. M. Olmstead, P. P. Power, *J. Am. Chem. Soc.* **2004**, *126*, 6510–6511.
- [11] H. Cox, P. B. Hitchcock, M. F. Lappert, L. J. M. Pierssens, *Angew. Chem. Int. Ed.* **2004**, *43*, 4500–4504; *Angew. Chem.* **2004**, *116*, 4600–4604.
- [12] K. Takeuchi, M. Ichinohe, A. Sekiguchi, *J. Am. Chem. Soc.* **2011**, *133*, 12478–12481.
- [13] a) A. Hinz, A. Schulz, A. Villinger, *Angew. Chem. Int. Ed.* **2015**, *54*, 668–672; *Angew. Chem.* **2015**, *127*, 678–682; b) S. Demeshko, C. Godemann, R. Kuzora, A. Schulz, A. Villinger, *Angew. Chem. Int. Ed.* **2013**, *52*, 2105–2108; *Angew. Chem.* **2013**, *125*, 2159–2162; c) T. Beweries, R. Kuzora, U. Rosenthal, A. Schulz, A. Villinger, *Angew. Chem. Int. Ed.* **2011**, *50*, 8974–8978; *Angew. Chem.* **2011**, *123*, 9136–9140; d) J. Bresien, A. Schulz, L. S. Szych, A. Villinger, R. Wustrack, *Dalton Trans.* **2019**, *48*, 11103–11111.
- [14] a) A. Schulz, *Dalton Trans.* **2018**, *47*, 12827–12837; b) A. Hinz, A. Schulz, A. Villinger, *Angew. Chem. Int. Ed.* **2016**, *55*, 12214–12218; *Angew. Chem.* **2016**, *128*, 12402–12406; c) A. Hinz, A. Schulz, A. Villinger, *Chem. Commun.* **2016**, *52*, 6328–6331.
- [15] a) J. Wen, Z. Havlas, J. Michl, *J. Am. Chem. Soc.* **2015**, *137*, 165–172; b) H. G. Viehe, Z. Janousek, R. Merenyi, L. Stella, *Acc. Chem. Res.* **1985**, *18*, 148–154.
- [16] a) K. Ota, R. Kinjo, *Chem. Soc. Rev.* **2021**, *50*, 10594–10673; b) H. Matsui, K. Fukuda, S. Takamuku, A. Sekiguchi, M. Nakano, *Chem. Eur. J.* **2015**, *21*, 2157–2164; c) I. Fernández, G. Frenking, G. Merino, *Chem. Soc. Rev.* **2015**, *44*, 6452–6463; d) V. Y. Lee, A. Sekiguchi, *Angew. Chem. Int. Ed.* **2007**, *46*, 6596–6620; *Angew. Chem.* **2007**, *119*, 6716–6740.
- [17] B. Braïda, A. Lo, P. C. Hiberty, *ChemPhysChem* **2012**, *13*, 811–819.
- [18] T. Stuyver, D. Danovich, S. Shaik, *J. Phys. Chem. A* **2019**, *123*, 7133–7141.
- [19] Z. Li, X. Chen, D. M. Andrada, G. Frenking, Z. Benko, Y. Li, J. R. Harmer, C. Y. Su, H. Grützmacher, *Angew. Chem. Int. Ed.* **2017**, *56*, 5744–5749; *Angew. Chem.* **2017**, *129*, 5838–5843.
- [20] D. Rottschäfer, B. Neumann, H.-G. Stämmler, R. S. Ghadwal, *Chem. Eur. J.* **2017**, *23*, 9044–9047.
- [21] R. S. Ghadwal, *Acc. Chem. Res.* **2022**, *55*, 457–470.
- [22] Deposition Numbers 2168117 (for **2**), 2168122 (for **4**), 2168118 (for **5a**), 2168119 (for **6**), 2168121 (for **7**), and 2168120 (for **8**) contain the supplementary crystallographic data for this paper. These data are provided free of charge by the joint Cambridge Crystallographic Data Centre and Fachinformationszentrum Karlsruhe Access Structures service.
- [23] M. Y. Abraham, Y. Wang, Y. Xie, P. Wei, H. F. Schaefer III, P. v. R. Schleyer, G. H. Robinson, *Chem. Eur. J.* **2010**, *16*, 432–435.
- [24] S. M. Ibrahim Al-Rafia, A. C. Malcolm, S. K. Liew, M. J. Ferguson, R. McDonald, E. Rivard, *Chem. Commun.* **2011**, *47*, 6987–6989.
- [25] a) R. S. Ghadwal, C. J. Schürmann, D. M. Andrada, G. Frenking, *Dalton Trans.* **2015**, *44*, 14359–14367; b) R. S. Ghadwal, C. J. Schürmann, F. Engelhardt, C. Steinmetzger, *Eur. J. Inorg. Chem.* **2014**, 4921–4926.
- [26] D. Rottschäfer, T. Glodde, B. Neumann, H. G. Stämmler, D. M. Andrada, R. S. Ghadwal, *Angew. Chem. Int. Ed.* **2021**, *60*, 15849–15853; *Angew. Chem.* **2021**, *133*, 15983–15987.
- [27] a) P. Pyykkö, M. Atsumi, *Chem. Eur. J.* **2009**, *15*, 12770–12779; b) M. Mantina, A. C. Chamberlin, R. Valero, C. J. Cramer, D. G. Truhlar, *J. Phys. Chem. A* **2009**, *113*, 5806–5812.
- [28] a) M. K. Sharma, S. Blomeyer, B. Neumann, H. G. Stämmler, R. S. Ghadwal, *Chem. Eur. J.* **2019**, *25*, 8249–8253; b) M. K. Sharma, S. Blomeyer, B. Neumann, H.-G. Stämmler, M. van Gastel, A. Hinz, R. S. Ghadwal, *Angew. Chem. Int. Ed.* **2019**, *58*, 17599–17603; *Angew. Chem.* **2019**, *131*, 17763–17767.
- [29] a) G. Frenking, M. Hermann, D. M. Andrada, N. Holzmann, *Chem. Soc. Rev.* **2016**, *45*, 1129–1144; b) L. Zhao, M. Hermann, N. Holzmann, G. Frenking, *Coord. Chem. Rev.* **2017**, *344*, 163–204; c) L. Zhao, S. Pan, N. Holzmann, P. Schwerdtfeger, G. Frenking, *Chem. Rev.* **2019**, *119*, 8781–8845; d) K. Ota, R. Kinjo, *Chem* **2022**, *8*, 340–350.
- [30] a) M. Nakano, R. Kishi, N. Nakagawa, S. Ohta, H. Takahashi, S.-i. Furukawa, K. Kamada, K. Ohta, B. Champagne, E. Botek, S. Yamada, K. Yamaguchi, *J. Phys. Chem. A* **2006**, *110*, 4238–4243; b) K. Yamaguchi, M. Okumura, K. Takada, S. Yamana-ka, *Int. J. Quantum Chem.* **1993**, *48*, 501–515.
- [31] Note, however, NICS and ACID magnetic criteria cannot completely rule out the multifaceted aromatic character of **6**.
- [32] a) M. K. Sharma, F. Ebeler, T. Glodde, B. Neumann, H.-G. Stämmler, R. S. Ghadwal, *J. Am. Chem. Soc.* **2021**, *143*, 121–125; b) M. K. Sharma, D. Rottschäfer, T. Glodde, B. Neumann, H. G. Stämmler, R. S. Ghadwal, *Angew. Chem. Int. Ed.* **2021**, *60*, 6414–6418; *Angew. Chem.* **2021**, *133*, 6485–6489.
- [33] M. K. Sharma, B. Neumann, H.-G. Stämmler, D. M. Andrada, R. S. Ghadwal, *Chem. Commun.* **2019**, *55*, 14669–14672.
- [34] I. Vránová, V. Kremláček, M. Erben, J. Turek, R. Jambor, A. Růžička, M. Alonso, L. Dostál, *Dalton Trans.* **2017**, *46*, 3556–3568.

Manuscript received: May 19, 2022

Accepted manuscript online: June 2, 2022

Version of record online: July 13, 2022